Adipocyte 1:3, 142–152; July/August/September 2012; © 2012 Landes Bioscience

Haptoglobin deficiency determines changes in adipocyte size and adipogenesis

Olimpia Gamucci,[1] Simonetta Lisi,[1,2] Gaia Scabia,[1,2] Matilde Marchi,[1,2] Paolo Piaggi,[3] Emiliano Duranti,[4] Agostino Virdis,[4] Aldo Pinchera,[1] Ferruccio Santini[1,*] and Margherita Maffei[1,2,5,*]

[1]Department of Endocrinology and Kidney; University-Hospital of Pisa; Pisa, Italy; [2]Dulbecco Telethon Institute; Pisa, Italy; [3]Department of Energy and Systems Engineering; University of Pisa; Pisa, Italy; [4]Department of Internal Medicine; University-Hospital of Pisa; Pisa, Italy; [5]Institute of Food Science; CNR; Avellino, Italy

Keywords: haptoglobin, size, adipogenesis, high fat diet, development

Abbreviations: WAT, white adipose tissue; HFD, high fat diet; CFD, chow food diet; WT, wild type; $Hp^{-/-}$, haptoglobin deficient, EPI, epididymal; SC, subcutaneous; SVF, stromal vascular fraction; FAS, fatty acid synthase; LPL, lipoprotein lipase; FABP-4/aP2, adipose fatty acid binding protein-4; PPARγ, peroxisome proliferator-activated receptor gamma; HSL, hormone sensitive lipase; VEGF, vascular endothelial growth factor; TIE1, tyrosine kinase with immunoglobulin-like and EGF-like domains 1; PECAM, platelet/endothelial cell adhesion molecule 1; C/EBP, CCAAT-enhancer-binding protein

Haptoglobin (Hp) is an inflammatory and adiposity marker, its expression during obesity being specifically induced in the white adipose tissue (WAT). We previously reported that when challenged with a high fat diet (HFD) $Hp^{-/-}$ mice are partially protected from the onset of insulin resistance and hepatosteatosis. The aim of the present study was to get further insights into Hp function in WAT. To this end, we performed histological and gene expression analysis of the $Hp^{-/-}$ WAT, both in standard and obesity conditions, and investigated how Hp deficiency impacts adipogenesis and WAT development.

The average size and percentage of very large adipocytes were respectively smaller and reduced in HFD $Hp^{-/-}$ mice as compared with HFD WT. The expression of perilipin, HSL and angiogenesis related markers were increased in HFD $Hp^{-/-}$ mice. Lean adult $Hp^{-/-}$ showed significantly larger adipocytes and lower subcutaneous WAT expression of *aP2* and *LPL* with respect to WT. $Hp^{-/-}$ young mice (P30) were characterized by larger adipocyte size and lower expression of adipocyte and adipogenesis markers. Comparison of adipocyte size distribution between young and adult mice revealed attenuated changes in $Hp^{-/-}$ mice compared with WT. Mouse embryonic fibroblasts from $Hp^{-/-}$ mice were less capable of accumulating triglycerides and exhibited lower expression of *PPARγ*, *aP2*, *FAS*, *LPL* and *Leptin*.

In conclusion, Hp deficiency tends to blunt the effect of age and diet on the size of adipocytes, which show less susceptibility to develop hypertrophy during obesity and a reduced adipogenic/hyperplastic potential during youth. In addition, Hp deficiency impacts negatively on adipogenesis.

Introduction

Haptoglobin (Hp) is among those genes that mark the intersection between obesity and inflammation. Classically known as a glycoprotein involved in the liver acute phase response to inflammation,[1] Hp is also highly expressed in the white adipose tissue (WAT),[2] its expression therein as well as its circulating levels being significantly related to the degree of adiposity.[3,4] One of Hp's most important functions is to bind free hemoglobin (Hb), thus preventing its oxidant activity.[5] At tissue level, angiogenic properties have been attributed to this protein and we recently reported that Hp also possesses a chemotactic activity, as it is able to attract monocytes by interacting with the C-C chemokine receptor 2 (CCR2).[6]

The biological significance of these observations was partly found in the characterization of the Hp deficient mouse ($Hp^{-/-}$) metabolic phenotype that we recently reported:[7] this mouse does not display any overt phenotype in standard feeding conditions. When exposed to high fat diet (HFD), despite susceptibility to weight gain similar to wild type (WT) mice, $Hp^{-/-}$ mice are partly protected from the onset of two serious obesity co-morbidities: namely insulin resistance and hepatosteatosis. The WAT of the obese $Hp^{-/-}$ mouse is not altered in its gross morphology, but displays interesting changes that likely contribute to its benign phenotype, including increased expression of adiponectin and decreased macrophage infiltration, the latter being well consistent with the chemotactic potential of Hp and with the widely accepted concept that the massive macrophage infiltration observed in the WAT of obese individuals is a determinant of their enhanced systemic inflammation and in turn a cause of insulin resistance, fatty liver and atherosclerosis.[8] Therefore, the metabolic phenotype of the $Hp^{-/-}$ mouse supports

*Correspondence to: Margherita Maffei and Ferruccio Santini; Email: mmaffei@dti.telethon.it and ferruccio.santini@med.unipi.it
Submitted: 12/07/11; Revised: 03/15/12; Accepted: 03/15/12
http://dx.doi.org/10.4161/adip.20041

the notion that WAT, just like any other endocrine organ, may orchestrate several functions of the organism through changes that pertain to its gene expression. These changes often take place during obesity. Hp upregulation observed in obesity is specific of WAT,[3] not being observed in other organs like liver[7] or lung.

Other examples of inflammatory molecules expressed in the WAT include: TNF-α, IL-6 and MCP-1. The role of these factors in adipocyte biology has been investigated through various approaches. A positive association between adipocyte diameter and IL-6 and TNF-α levels has been described in humans.[9] Impairment of TNF-α signaling resulted in smaller adipocyte size both in standard and obesity conditions.[10] When exposed to high fat diet MCP-1 deficient mice undergo a less pronounced enlargement of their adipocytes as compared with wild type. Conversely, IL-6 deficiency results in fat mass and adipocyte size increase.[11] In vitro adipogenesis is negatively regulated by TNF-α,[12] while MCP-1 treatment of 3T3-L1 cells induces adipocyte marker expression and promotes adipose conversion.[13]

Differently from the inflammatory markers mentioned above, which are extensively present in other cell types, Hp expression is confined to the adipocyte fraction.[3] Fain reported that Hp is released by explants of human adipose tissue, both by isolated adipocytes and adipose tissue matrix, but not by cells of the stromal vascular fraction (SVF).[14] These results are in agreement with the observation by Do Nascimento et al.,[15] who showed that in murine adipose tissue Hp is one of those few inflammatory molecules specifically produced by the adipocytes and not present in the SVF.

Based on the outlined concepts, we wanted to further understand how Hp deficiency impacts WAT in terms of adipocyte size, gene expression and adipogenic potential. Our findings indicate that $Hp^{-/-}$ WAT reacts differently to the hypertrophic phase that characterizes obesity and to the hyperplastic phase typical of the peri-weaning period.[16] Further, an impaired adipogenic potential was observed in $Hp^{-/-}$ embryonic fibroblasts.

Results

Effect of HFD on physical parameters and adipose tissue histomorphology in the $Hp^{-/-}$ mouse. $Hp^{-/-}$ and WT mice were exposed to HFD for 12 weeks. No genotype related differences were evidenced in the susceptibility to gain weight, in WAT weight/body weight (% of fat) or food intake (**Fig. 1A–C**). As shown in **Figure 1D** the average adipocyte size of SC WAT of $Hp^{-/-}$ HFD treated animals was significantly smaller than that found in HFD WT mice. The $Hp^{-/-}$ EPI WAT exhibited similar features, albeit with less pronounced differences. Consistently, DNA content, an indirect assessment of adipocyte number, was higher (albeit not significantly) in both SC and EPI WAT from $Hp^{-/-}$ mice as compared with WT (**Fig. 1E**). Analysis of distribution of adipocyte size in SC WAT of obese animals indicated that Hp deficiency was associated with a higher number of small-sized adipocytes and a lower number of large-sized adipocytes as compared with WT (**Fig. 1F**).

Taken together these data indicate that, despite no difference in body weight and percentage of fat, obese Hp deficient mice show a reduced adipocyte size.

Adipocyte size in the lean $Hp^{-/-}$ mouse: comparison with the obese. In contrast to HFD-fed,[7] $Hp^{-/-}$ mice, no changes in systemic metabolism, and local inflammatory profile of WAT were observed in lean $Hp^{-/-}$ mouse compared with WT mice, suggesting that the role of Hp in metabolism and adipose tissue is more evident in the presence of a metabolic challenge. Percentage of fat was similar in WT and $Hp^{-/-}$ mice (**Fig. 2A**).

In the effort to understand if signs of the adipocyte related changes encountered in the HFD $Hp^{-/-}$ mice were somewhat anticipated under normal conditions we analyzed WAT of lean animals. Histological examination of WAT surprisingly revealed a larger adipocyte size of $Hp^{-/-}$ mice in both SC and EPI WAT (**Fig. 2B**), as opposed to what was found in obese mice. In this case, DNA content, was lower (albeit not significantly) in both SC and EPI WAT from $Hp^{-/-}$ mice as compared with WT (**Fig. 2C**). Consistently, adipocyte size distribution (represented in **Fig. 2D** for SC WAT) of CFD $Hp^{-/-}$ revealed a decreased number of relatively small/medium-sized adipocytes and an increased number of larger adipocytes.

The opposite trend in adipocyte size shown by obese and lean $Hp^{-/-}$ mice was unexpected and is suggestive of a diet effect acting differently in the WT and $Hp^{-/-}$ model. Indeed, when the diet effect (CFD-HFD) is plotted intra-genotype (**Fig. 2E and F**) a less pronounced enlargement of the bell shaped curve (black bars) describing the SC adipocyte size distribution can be seen for HFD $Hp^{-/-}$ as compared with HFD WT mice, indicating a reduced fluctuation of size in the former. While a good extent of overlapping is in fact present in the distribution of adipocyte size between lean and obese $Hp^{-/-}$ mice, diet change determines an almost complete separation of the distributions in the WT mouse.

Hp deficiency and WAT gene expression. To investigate the molecular mechanisms underlying the herein observed phenotypic differences and get further insights into the role of Hp in WAT, the expression of genes relevant for four functional categories, including adipocyte size, terminal differentiation, proliferation and angiogenesis, were investigated.

The size of individual adipocytes is mainly defined by triglyceride (TG) content that is hydrolyzed during lipolysis to glycerol and fatty acids.[17] To investigate the molecular mechanisms underlying size related difference we monitored the expression of *Perilipin* and hormone sensitive lipase (*HSL*), two key regulators of TG hydrolysis.[18,19] A modest downregulation of perilipin and HSL was observed in the SC WAT of CFD $Hp^{-/-}$ mice as compared with controls (**Fig. 3A**), In the EPI, but not in the SC WAT of HFD $Hp^{-/-}$ smaller size of adipocytes was accompanied by a significantly increased expression of *HSL* and a trend toward an increase of *Perilipin* (**Fig. 3B**).

Genes defining mature adipocytes, including fatty acid synthase (*FAS*), lipoprotein lipase (*LPL*), adipose fatty acid binding protein-4 (*FABP-4/aP2*) and peroxisome proliferator-activated receptor gamma (*PPARγ*) were also analyzed. A significantly lower expression of *LPL, aP2, PPARγ* was found in the SC WAT of CFD $Hp^{-/-}$ mice (**Fig. 3C**) as compared with CFD WT. No genotype related differences were found in HFD mice (**Fig. 3D**).

Difference in adipocyte size may be accompanied by differences in proliferation rate of progenitor cells (preadipocytes). To address

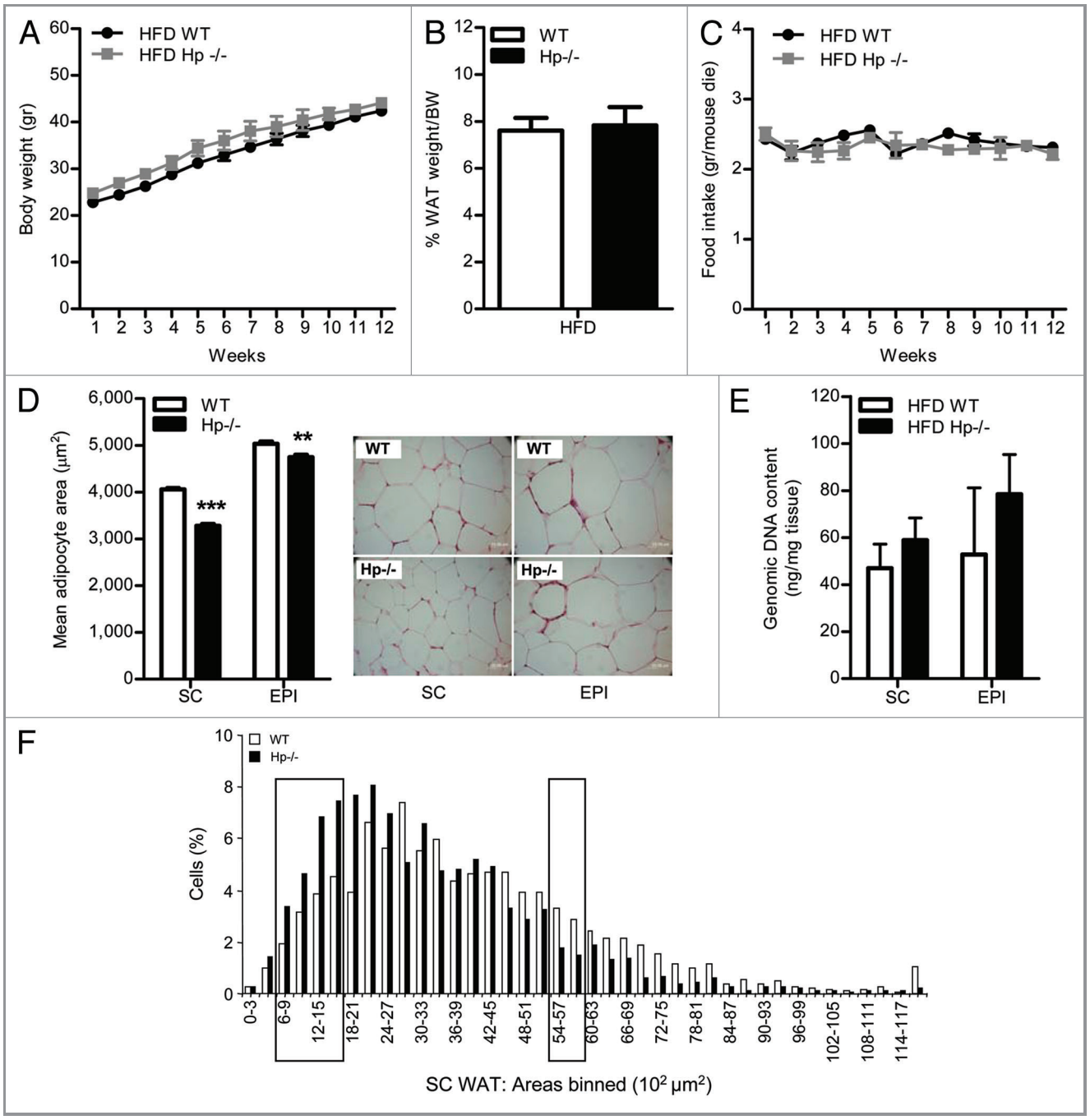

Figure 1. Effect of HFD on physical parameters and adipose tissue histomorphology in the $Hp^{-/-}$ mouse. (A) Body weight during HFD ($Hp^{-/-}$, gray squares, WT, black circles). (B) Fat % (PERI WAT weight + EPI WAT weight + SC WAT weight)/body weight) at the end of HFD. (C) Food intake of $Hp^{-/-}$ (gray squares) and WT (black circles) during HFD. (D) Left, bar graph showing the mean adipocyte area (μm^2) in the SC and EPI WAT of HFD WT and HFD $Hp^{-/-}$ mice (n = 4 for both genotypes and tissues). Right, representative histological sections of SC and EPI WAT of HFD WT and HFD $Hp^{-/-}$ mice. Mean weight of these fat depots was 1.48 ± 0.31 and 1.59 ± 0.17 g for WT and $Hp^{-/-}$ respectively for SC WAT and 1.67 ± 0.99 and 1.65 ± 0.69 for WT and $Hp^{-/-}$ respectively for EPI WAT. (E) Bar graph showing DNA content in the SC and EPI WAT of HFD WT and HFD $Hp^{-/-}$ mice (n = 5 for both genotypes and tissues). (F) Morphometric analysis of adipocyte cell size distribution (based on a total of about 2000 cells/genotype) of SC WAT in HFD WT and HFD $Hp^{-/-}$ mice (n = 4 for each genotype). Adipocyte areas are binned according to the genotype (each bin = 300 μm^2) and data are expressed as % of cells per bin. Black rectangles indicate bins in which the comparison between genotypes is significant (chi-square test, $p < 0.05$). Data are expressed as means ± SEM. For pair comparisons in (D), Student's t-test, $^{**}p < 0.01$, $^{***}p < 0.001$.

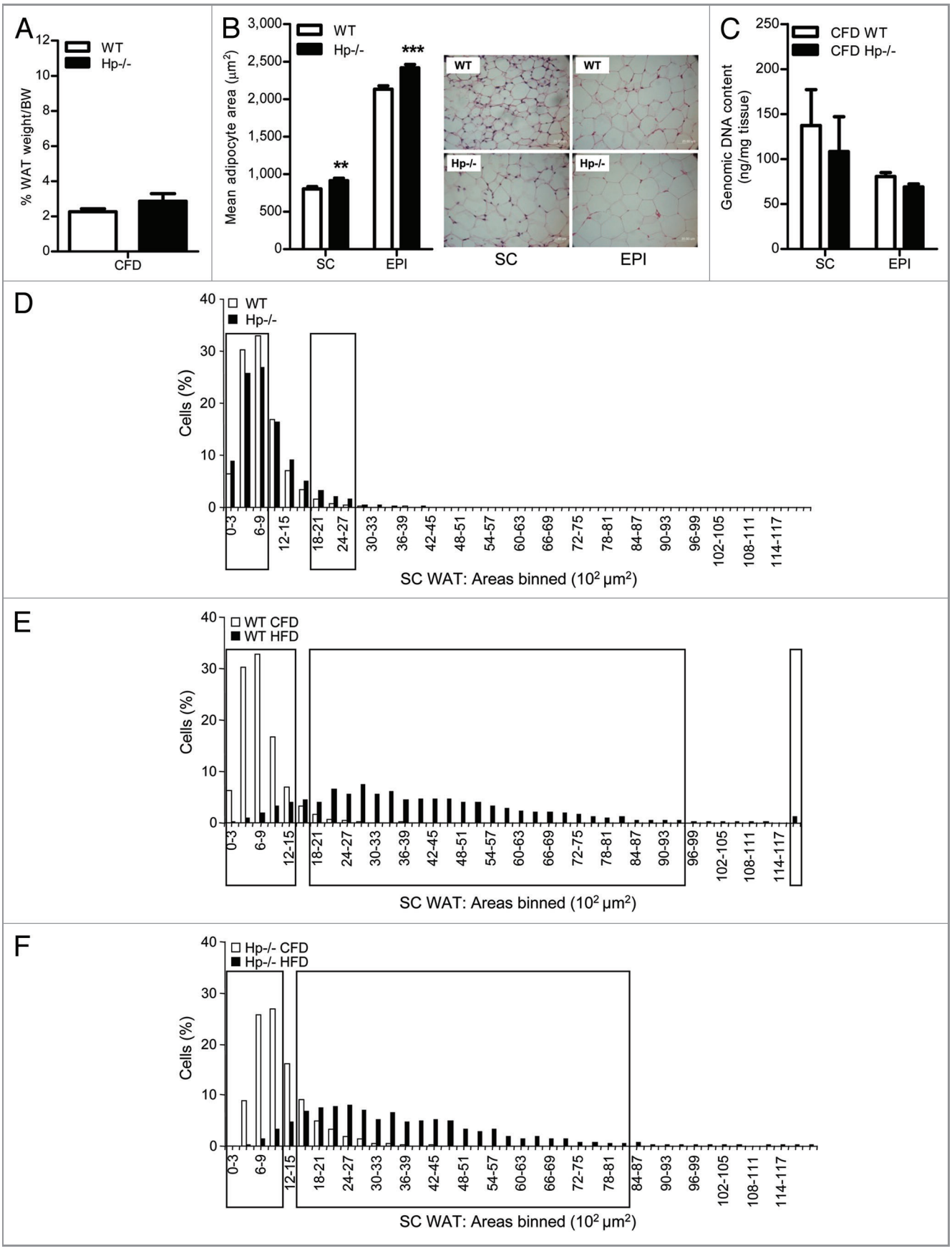
A
% WAT weight/BW
WT
Hp-/-
CFD
B
Mean adipocyte area (μm²)
WT
Hp-/-
**
***
SC
EPI
WT
WT
Hp-/-
Hp-/-
SC
EPI
C
Genomic DNA content (ng/mg tissue)
CFD WT
CFD Hp-/-
SC
EPI
D
Cells (%)
WT
Hp-/-
SC WAT: Areas binned (10² μm²)
E
Cells (%)
WT CFD
WT HFD
SC WAT: Areas binned (10² μm²)
F
Cells (%)
Hp-/- CFD
Hp-/- HFD
SC WAT: Areas binned (10² μm²)

Figure 2 (See previous page). WAT histomorphology in the lean $Hp^{-/-}$ mouse: comparison with the obese. (A) Fat % in CFD WT and $Hp^{-/-}$ mice. (B) Left, bar graph showing the mean adipocyte area (μm^2) in the SC and EPI WAT of CFD WT and CFD $Hp^{-/-}$ mice (n = 4 for both genotypes and tissues). Right, representative histological sections of SC and EPI WAT of CFD WT and CFD $Hp^{-/-}$ mice. Mean weight of these fat depots was 0.14 ± 0.03 and 0.16 ± 0.04 g for WT and $Hp^{-/-}$ respectively for SC WAT and 1.67 ± 0.99 and 1.65 ± 0.69 for WT and $Hp^{-/-}$ respectively for EPI WAT. (C) Bar graph showing DNA content in the SC and EPI WAT of CFD WT and HFD $Hp^{-/-}$ mice (n = 5 for both genotypes and tissues). (D) Morphometric analysis of adipocyte cell size distribution (based on a total of about 2,000 cells/genotype) of SC WAT in CFD WT and CFD $Hp^{-/-}$ mice (n = 4 for each genotype). Adipocyte areas are binned according to the genotype (each bin = 300 μm^2) and data are expressed as % of cells per bin. (E and F) Intra-diet morphometric analysis of adipocyte cell size distribution (based on a total of about 2000 cells/genotype) of SC WAT in WT (E) and $Hp^{-/-}$ (F) CFD and HFD mice (n = 4 for each genotype). Adipocyte areas are binned according to the diet (each bin = 300 μm^2) and data are expressed as % of cells per bin for both diet regimens. For (A–C) data are expressed as means ± SEM. Pair comparisons in (B), Student's t test, $^{**}p < 0.01$, $^{***}p < 0.001$. For (D–F) black rectangles indicate bins in which the comparison between genotypes (D) and diet regimens (E and F) is significant (chi-square test, $p < 0.05$).

this issue, we monitored the expression of genes regulating proliferation, including positive regulators c-*myc, c-fos, c-jun* and negative regulator, *Jun B*. In CFD mice, we found only a difference for *c-myc* and *Jun B* (not significant), respectively down- and upregulated in the $Hp^{-/-}$ SC WAT (**Fig. 3E**). No genotype-related significant differences were found in the obese mice with the exception of *c-Fos*, which was upregulated in the SC WAT of HFD $Hp^{-/-}$ mice as compared with HFD WT (**Fig. 3F**).

In the obesity setting, WAT needs an increase in blood flow and new vessel formation to prevent hypoxia. Given the angiogenic properties attributed to Hp,[20] we wanted to monitor the abundance of endothelial markers [tyrosine kinase with immunoglobulin-like and EGF-like domains 1 (*TIE1)*, platelet/endothelial cell adhesion molecule 1 (*PECAM*) and vascular endothelial growth factor (*VEGF*)], upon Hp deficiency. A slight reduction of *TIE1* was observed in the SC WAT of CFD $Hp^{-/-}$ mice (**Fig. 3G**, left panel). Surprisingly, an upregulation of both *TIE1* and *PECAM* was observed in the EPI WAT of HFD $Hp^{-/-}$ mice. *VEGF* abundance was upregulated both in the SC and EPI WAT of HFD $Hp^{-/-}$ as compared with HFD WT (**Fig. 3H**).

Taken together these data suggest that Hp deficiency affects WAT gene expression in different manners in both lean and obese mice. In the former, the most evident effect is a decreased abundance of terminal differentiation markers, while in the latter, increased activation of the lipolysis machinery and upregulation of angiogenesis related genes appear as the most relevant consequences.

Hp and adipogenesis. Given the widely accepted concept that adipogenesis may contribute to the enlargement of adipose mass during obesity, we asked whether a different capacity to undergo de novo adipose conversion might contribute to the different WAT histological phenotype seen in HFD WT and HFD $Hp^{-/-}$ mice.

As previously reported by others, Hp mRNA increases during adipose conversion.[21] To further investigate if this adipogenesis dependent regulation has functional implications, we isolated mouse embryonic fibroblasts (MEFs) from $Hp^{-/-}$ and WT mice. No genotype dependent difference in proliferation rate, as assessed by BrdU incorporation, was evidenced (not shown). When cells were treated with an adipogenic differentiation cocktail, $Hp^{-/-}$ MEFs showed a diminished capability to undergo adipogenesis as compared with MEFs from controls. This was revealed by less intense Oil Red O staining (**Fig. 4A**) and by significantly lower triglyceride content in $Hp^{-/-}$ MEFs as compared with WT MEFs (**Fig. 4B**). These results were confirmed by the significantly lower expression of terminal differentiation markers in $Hp^{-/-}$ as compared with WT MEFs (**Fig. 4C**). The expression of *Leptin*, *FAS*, *LPL* and *aP2* in $Hp^{-/-}$ MEFs at day 10 post cocktail induction (PCI) was respectively 47%, 41%, 68% and 38% that of WT MEFs. Interestingly, a significant difference in the expression of genes that orchestrate adipogenesis, including *PPARγ* and CCAAT/enhancer binding protein α (*C/EBPα*), was already evident at earlier time points of the differentiation process. As evidenced in **Figure 4D**, $Hp^{-/-}$ MEFs showed a lower *PPARγ* expression at various time points PCI. *C/EBPα* showed a similar trend (**Fig. 4E**), even if statistically significant only at day 4.

These results indicate that MEFs from $Hp^{-/-}$ mice are less prone to undergo adipose conversion and to store triglycerides.

$Hp^{-/-}$ WAT in the developing animal. Although in vitro differentiation of MEFs does not fully recapitulate what takes place in vivo, our results rule out de novo adipogenesis as a mechanism to explain the reduced adipocyte size found in obese $Hp^{-/-}$ mice. We then wanted to get further in vivo insights on this issue during growth in the peri-weaning period, when upon diet change (from breast to autonomous feeding) the adipose mass enlarges and an increase in both adipocyte number and size is required.[16]

We analyzed body fat in $Hp^{-/-}$ and WT mice at postnatal day (P) 30. Weight of SC and EPI WAT did not differ between $Hp^{-/-}$ and WT mice (**Fig. 5A**). Morphometric analysis performed in SC and EPI WAT revealed a greater cell size in $Hp^{-/-}$ mice as compared with WT, in line with what was observed in the adult animal (**Fig. 5B**). Consistently, cell surface distribution (herein shown for SC WAT, **Fig. 5C**) highlighted a lower and higher number of respectively very small and large adipocytes in $Hp^{-/-}$ mice. When age dependent changes (P30 and adult) were evidenced through an intra-genotype plot (**Fig. 5D and E**), we observed a lower percentage of small cells (0–600 μm^2) in the $Hp^{-/-}$ as compared with the WT in P30 mice (white line, circles). Further, upon adulthood (3–5 mo of age, black line, circles) this number was reduced in WT, whereas it remained unchanged in the $Hp^{-/-}$ mouse.

Gene expression studies performed on young mice revealed a lower expression of adipocyte specific markers (*FAS*, *LPL*, *aP2* and *PPARγ*) in both the SC and EPI WAT (**Fig. 5F and G**), this being in line with what was found in the MEFs and in the lean adult mouse.

Taken together, these results indicate that features present in the adult $Hp^{-/-}$ WAT are already present in the newly formed adipose tissue of very young animals.

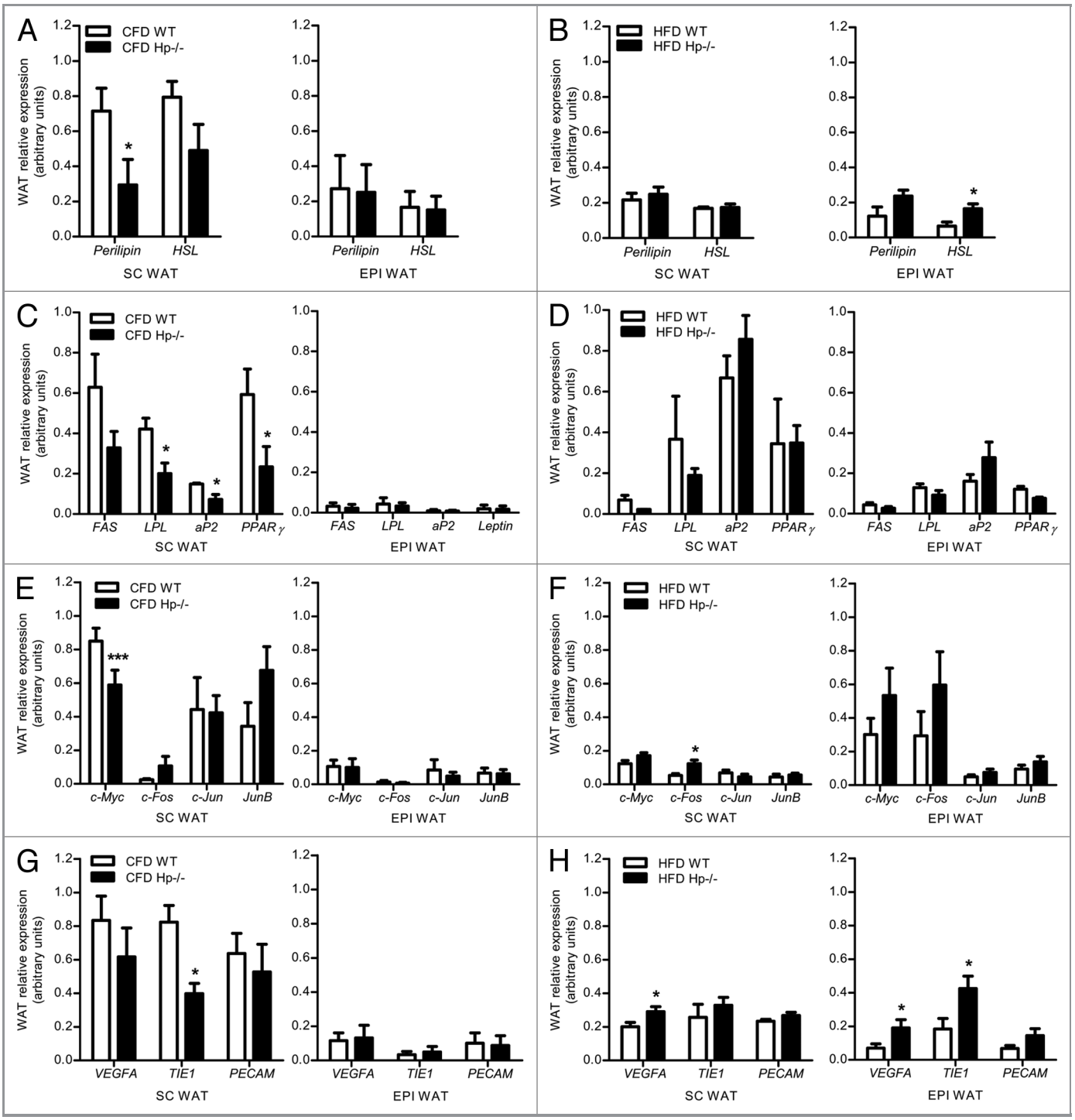

Figure 3. WAT gene expression upon Hp deficiency. Relative expression of *Perilipin* and *HSL* in WAT of CFD (A) and HFD (B) mice. Relative expression of *FAS, LPL, aP2* and *PPARγ* in WAT of CFD (C) and HFD (D) mice. Relative expression of *c-myc, c-fos, c-jun* and *Jun B* in WAT of CFD (E) and HFD (F) mice. Relative expression of *TIE1, PECAM* and *VEGF* in WAT of CFD (G) and HFD (H) mice. In left and right panels data relative to SC and EPI WAT are shown respectively. Data are expressed as means ± SEM, n = 4 for each group (i.e., SC CFD WT, SC CFD $Hp^{-/-}$, etc.). Pair comparisons, Student's t-test, *$p < 0.05$, ***$p < 0.001$.

Discussion

Findings presented herein indicate that obese $Hp^{-/-}$ mice have a smaller adipocyte size as compared with obese WT mice. Upon obesity, a protection against excessive size of adipocytes has been positively associated with increased insulin sensitivity and higher expression of adiponectin.[22,23] In line with this concept, we previously demonstrated that higher adiponectin production and

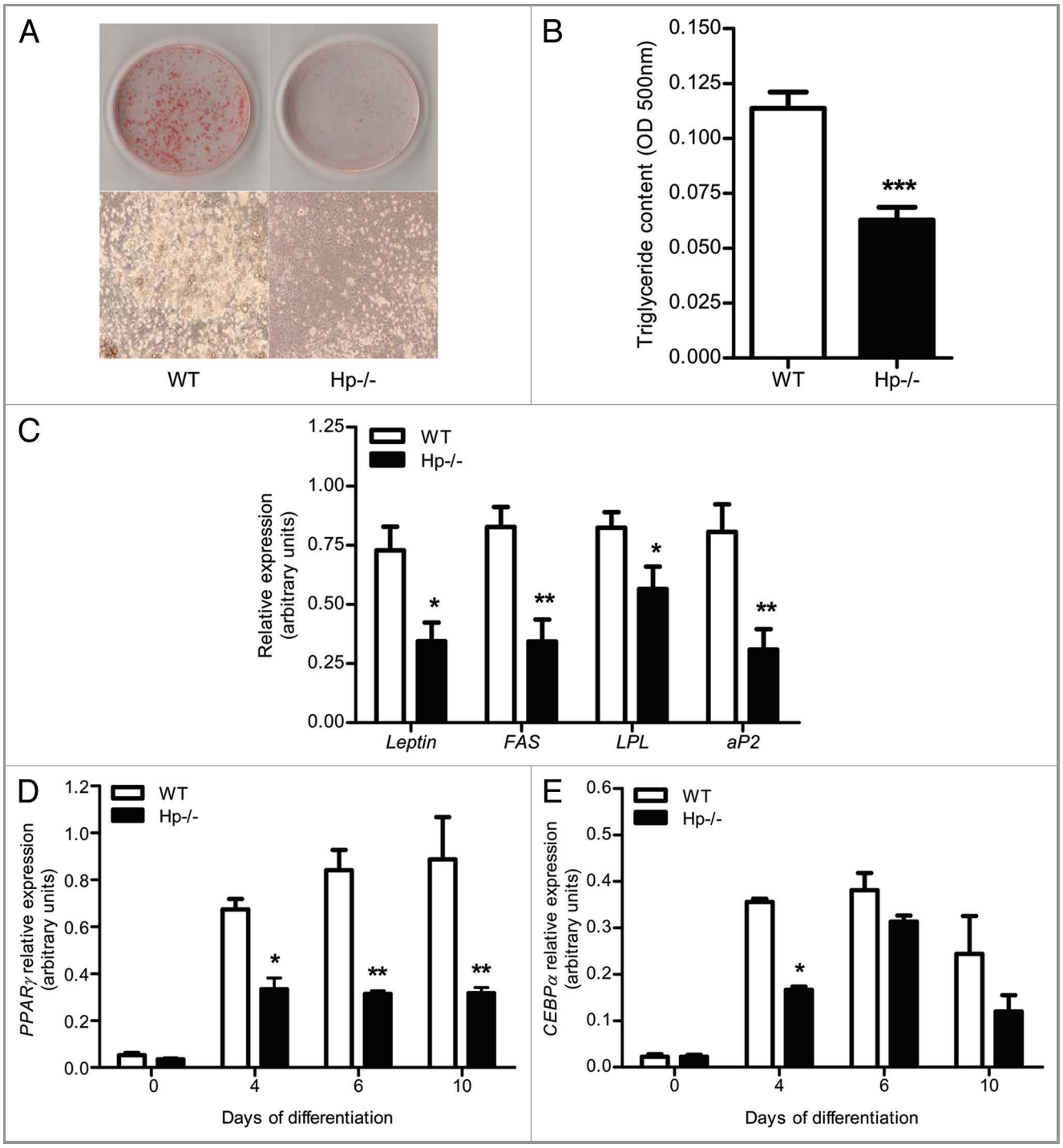

Figure 4. MEFs from $Hp^{-/-}$ mice show a diminished capability to undergo adipogenesis. (A) Oil Red O staining (upper panels) and representative images of cells (40× magnification, lower panels) in WT and $Hp^{-/-}$ MEFs at terminal differentiation (day 10). (B) Triglyceride content measurement in WT and $Hp^{-/-}$ MEFs at terminal differentiation (day 10). (C) *Leptin*, *FAS*, *LPL* and *aP2* relative expression at terminal differentiation (day 10) in WT and $Hp^{-/-}$ MEFs. *PPARγ* (D) and *CEBPα* (E) relative expression during adipose conversion in WT and $Hp^{-/-}$ MEFs. *PPARγ*: 2-way ANOVA, genotype effect $p < 0.0001$, time effect $p < 0.0001$, interaction $p < 0.05$. Bonferroni post-hoc tests: WT *vs* $Hp^{-/-}$ *$p < 0.05$, **$p < 0.01$. *CEBPα*: 2-way ANOVA, genotype effect $p < 0.001$, time effect $p < 0.0001$. Bonferroni post-hoc test: WT *vs* $Hp^{-/-}$ *$p < 0.05$. Data are expressed as means ± SEM. For pair comparisons in (B and C) Student's t-test, *$p < 0.05$, **$p < 0.01$, ***$p < 0.001$.

insulin-dependent AKT activation defines WAT as a key element in the protection against the obesity associated onset of systemic insulin resistance in the $Hp^{-/-}$ model.[7] In the context of the present study we also found an increased activation of the TG hydrolysis machinery and an augmented expression of endothelial markers.

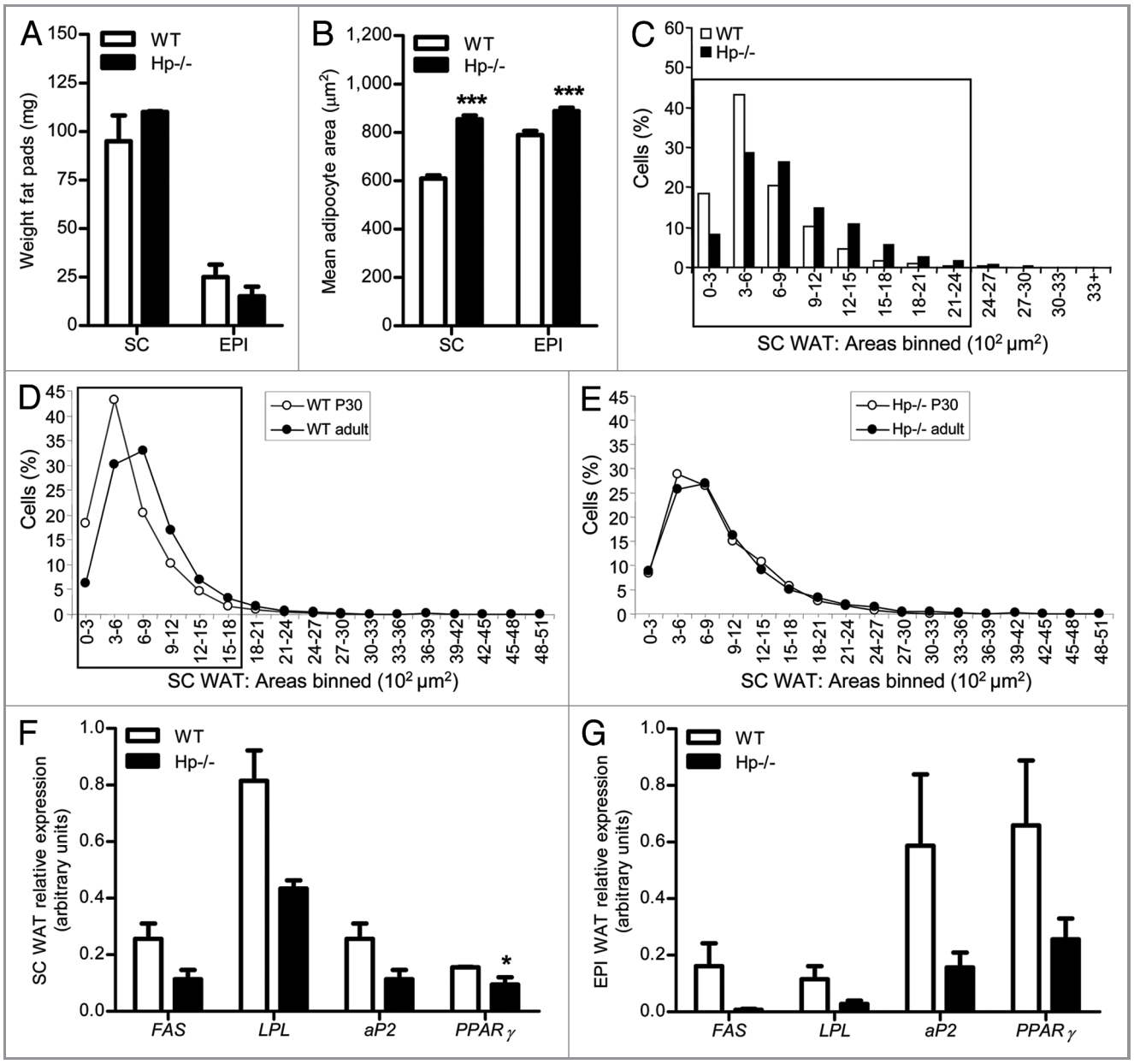

Figure 5. Weight, adipocyte size and gene expression in the WAT of developing $Hp^{-/-}$ mouse. (A) Weight of SC and EPI fat depots of P30 WT and $Hp^{-/-}$ mice (n = 3). (B) Bar graph showing the mean adipocyte area (μm^2) in the SC and EPI WAT of P30 WT and $Hp^{-/-}$ mice. (C) Morphometric analysis of adipocyte cell size distribution (based on a total of about 2,500 cells/genotype) of SC WAT in P30 WT and $Hp^{-/-}$ mice. Adipocyte areas are binned according to the genotype (each bin = 300 μm^2) and data are expressed as % of cells per bin. Black rectangle indicates bins in which the comparison between genotypes is significant (chi-square test, $p < 0.05$). (D and E) Morphometric analysis of adipocyte cell size distribution of SC WAT of P30 and adult WT (D) and $Hp^{-/-}$ (E) mice. Data are expressed as % of cells per bin. Black rectangle indicates bins in which the comparison between ages is significant [chi-square test, $p < 0.001$ for (D)]. (F and G) *FAS, LPL, aP2* and *PPARγ* relative expression in SC (F) and EPI (G) WAT of P30 WT and $Hp^{-/-}$ mice (WT n = 3, $Hp^{-/-}$ n = 2). Data are expressed as means ± SEM. For pair comparisons in (B) and (F), Student's t test, *$p < 0.05$, ***$p < 0.001$.

All these data are therefore consistent with an Hp deficient phenotype that is partially protected from the onset of the metabolic derangements of obesity which appears to be associated with increased expression of the inflammatory molecule Hp. In this respect, it is of interest to compare our findings with those from Jo and colleagues,[24] who employed a sophisticated computational approach to the study of hypertrophy and hyperplasia of adipocytes in obesity resistant FVB and obesity susceptible C57BL/6J mice during regular CFD and HFD. Their results indicate that hypertrophy and not hyperplasia is a major determinant in the rapid enlargement of fat mass typical of HFD. Cell size growth moves the mode of the cell size distribution to larger sizes and increases the spread of the distribution around the mode. This effect is more pronounced in the C57BL/6J mice that become insulin resistant in response to HFD, as compared with the FVB that remain more insulin sensitive. Our intra-genotype

analyses, although not as accurate, revealed that in $Hp^{-/-}$ mice the cell size distribution spread, due to HFD, is attenuated as compared with WT, thus confirming a resistance to the effect of HFD, somewhat reminiscent of what takes place in the FVB strain. Further, within the EPI WAT, Hp, deficiency results in increased expression of *perilipin* and *HSL*. *Perilipin* is a key regulator of both lipid storage and lipolysis that anchors to the surface layer of the lipid droplet acting as an organizing center for lipid metabolic enzymes, thus triggering lipolysis and reduction of adipocyte size.[25] Interestingly, transgenic overexpression of *perilipin* resulted in improved glucose/insulin homeostasis in HFD treated mice, this potentially being linked to the improved glucose tolerance and insulin tolerance that we elsewhere reported for HFD $Hp^{-/-}$ mice.[7] Among the adverse obesity outcomes undergone by adipose tissue and attenuated by Hp deficiency, data herein presented allow us to include protection against reduced vascularization and blunted angiogenic potential. This phenomenon is, in fact, often found in obese individuals[26,27] and constitutes the structural premise for hypoxia and downstream consequences.[28]

In the lean $Hp^{-/-}$ mouse, we did not previously observe[7] any metabolic alteration and, in contrast to what takes place in the obesity condition, its WAT was characterized by larger adipocytes since youth (P30). This is a very crucial period for development of rodent adipose tissue, when diet changes from breast to autonomous feeding. Studies performed in rat by Herrera and colleagues indicate the period from birth to P40 as the phase with the highest hyperplasia, at the end of which an important hypertrophic phase begins (P40–P80).[16] In this regard, we previously reported that cathepsin K null mice, which do not present any body fat alteration during adulthood, exhibit a delay in the accumulation of fat stores that can be evidenced in this specific phase.[29] In the present study, cell size distribution mode (over 40%) of P30 WT is centered on the 300–600 μm^2 cell size, whereas in the Hp deficient animal the mode (less than 30%) is centered on larger cells (300–900 μm^2). In addition, WAT of young $Hp^{-/-}$ mice exhibits a lower expression of the key adipogenic orchestrator *PPARγ*. If analyzed through Herrera's paradigm, this means that Hp deficiency impairs the hyperplastic phase in favor of an anticipated hypertrophic phase of young adipocytes. Accordingly, data obtained in MEFs show a reduced capacity to be converted to adipocytes in the $Hp^{-/-}$ as compared with WT cells. It is therefore likely that at P30 adipogenesis is less active in the WAT of the $Hp^{-/-}$ mouse. Even more interesting is what emerges when the age effect (from P30 to adult) is plotted intra-genotype (**Fig. 5E**). Whereas cell size distribution of WT mice shows a shift of the distribution mode to a larger cell size (from 300–600 to 600–900 μm^2), with a significant reduction in the number of very small cells and an augmented percentage of large cells (> 900 μm^2, **Fig. 5D**), this shift in cell size distribution was attenuated in $Hp^{-/-}$ mice.

Lower expression of *LPL*, *FAS*, *aP2*, *PPARγ* and *c-myc* characterizes the lean adult $Hp^{-/-}$ WAT. Interestingly, lipogenic gene expression was reported to be inversely related to adipocyte size in humans and this was suggested to contribute to insulin resistance.[23] In our case, larger size does not correspond to any change in insulin-sensitivity in lean $Hp^{-/-}$ mice. In this regard it is worth noticing that in the study by Roberts and coworkers, both lean and obese subjects were recruited (BMI range 20–37), and when adipocyte size is plotted against HOMA-IS index, the resulting negative relationship is importantly triggered by very large adipocytes, likely deriving from obese subjects, that are not represented in our sample.

It is of interest to analyze our findings also through the innovative model proposed by Muller,[30] who speculates about the existence of signals sent by large adipocytes to order small adipocytes to "take-over" the excess of lipid loading. This should lead to the upregulation of lipid storage in small adipocytes and thus blunt the spread (small/large) of cell size within the tissue. If any, Hp action within this dialog has to be negative, given that both during obesity and growth, Hp deficiency attenuated the spread effect, implying that lipid storage is more homogeneously distributed among existing cells.

Overall, our findings suggest that in the absence of the anti-oxidant inflammatory-related factor Hp, the adipocyte size distribution tends to be more static both during the hyperplastic phase that characterizes the early stages of life and upon the HFD induced hypertrophy. While the impaired adipogenic potential observed in $Hp^{-/-}$ MEFs accounts for the former observation, the relationship with the latter is somewhat controversial. The role of adipogenesis in the onset/protection against obesity and associated comorbidities is being debated as exemplified by the following studies: the groucho family member transducin-like enhancer of split 3 (*TLE3*) is a potent facilitator of *PPARγ* activity and an adipogenic factor. Transgenic mice that overexpress this factor in WAT show an ameliorated insulin resistance upon HFD.[31] By contrast, an ameliorated glucose and fat metabolism is observed in mice that are deficient for phospholipase C (*PLC*) *δ1*, which also promotes adipogenesis.[32] De novo adipogenesis is not the only determinant of adipocyte size distribution, which is also importantly controlled by cell loss. Excessive size triggers a necrotic cell death phenomenon in obesity.[33,34] Further, enhanced oxidative stress (OS) has been implied in HFD-dependent cell death in adipose tissue.[35] This effect could be amplified by the lack of Hp, the main carrier of the potent oxidant free Hb. Although purely speculative, a possibility is that in the obese $Hp^{-/-}$ mouse, very large cells, more susceptible to die in normal conditions, are further selected negatively by high OS and become less represented in the population.

In conclusion, our data suggest that adipocytes from $Hp^{-/-}$ mice are less susceptible to become oversized during obesity. Further, Hp deficiency impairs adipose conversion of mouse embryonic fibroblasts, this being consistent with signs of less active adipogenesis shown by the lean young and adult $Hp^{-/-}$ mouse.

Materials and Methods

Experimental animals. The strategy used to target the Hp locus and generate $Hp^{-/-}$ mice was as previously described.[36] Age-matched littermates C57BL/6J wild type were used as controls. Adult mice were placed on either a CFD (Diet 2018 Teklad global diet, 18.9% protein, 5.7% fat and 57.3% g/weight

carbohydrate, Harlan Teklad) or on a HFD (Diet F3282, 19% protein, 36% fat and 35% carbohydrate g/weight, Bioserve). Food intake and BW were monitored as previously described.[7] Animals that did not reach 40 g of weight at the end of the diet were excluded from further investigations. No genotype-related difference was observed in the frequency of failure to become obese. SC (from the inguinal region), EPI and perirenal (PERI) WAT from adult and P30 mice were dissected, weighed, then frozen in liquid nitrogen for mRNA expression experiments or stored in formalin for histology. Fat % was calculated as follows: (weight of EPI WAT + weight of PERI WAT + weight of SC WAT)/body weight.

The experimental protocols followed the Principles of Laboratory Animal Care and a specific authorization was issued by Italian Ministry of Education (114/2003-A of 16/09/2003) to CNR Neuroscience Institute, where animals were housed.

Histological and morphometric analysis of tissues. SC and EPI WAT of adult and P30 mice were fixed in 10% formaldehyde and embedded in paraffin. Five-micrometer sections of paraffin-embedded samples were stained with H&E. At least 15 random optical fields per individual sample were acquired using a Nikon Eclipse i80 microscope (40X magnification). Adipocyte areas were determined using ImageJ software.

MEFs isolation, culture, proliferation rate and differentiation. Primary MEFs were isolated from embryos of WT and $Hp^{-/-}$ mice at 15 d post coitum. Embryos were surgically removed and separated from maternal tissue and yolk sack. The bodies were finely minced, washed in phosphate-buffered saline (PBS) and digested in a solution of 0.1% trypsin-EDTA with shaking at 37°C for 10 min. The solution was allowed to settle for 2 min and the supernatant was centrifuged for 3 min at 1200 rpm at 37°C. Cells were resuspended in Dulbecco's modified Eagle's medium (DMEM, Invitrogen 41965) supplemented with 10% heat-inactivated fetal bovine serum (FBS), 100 U/ml penicillin and 100 mg/ml streptomycin and plated at 10^4 cells/cm^2 at 37°C in 5% CO_2. All experiments were performed using cells at passage 3. Cell proliferation was measured using a commercial colorimetric BrdU incorporation based immunoassay (Roche Diagnostics 11647229001) following manufacturer's instructions.

For differentiation MEFs were allowed to reach confluence, and two days after (day 0) adipose conversion was induced by addition in the culture medium of an induction cocktail containing 1.67 μM insulin (Sigma-Aldrich, I-5500), 5 μM dexamethasone (DEXA, Sigma-Aldrich, D1756), 0.3 mM 3-isobutyl-1-methylxanthine (IBMX, Sigma-Aldrich, I7018) and 1 μM rosiglitazone (BRL-49653, kindly provided by Glaxo SmithKline). From day 2 post induction, cells were cultured with DMEM supplemented with only 1.67 μM insulin and 1 μM BRL, that was renewed every 2 d until terminal differentiation (day 10). Pictures of differentiated cells were taken using a Leica microscope (40× magnification).

Oil Red O staining. Oil Red O staining was performed at the end of MEFs differentiation process (day 10). Cells were washed twice with PBS and fixed with 3.7% formaldehyde (Sigma-Aldrich, F8775) in PBS for 1 h at room temperature (RT). Cells were then washed three times with deionized water and stained with filtered Oil Red O working solution [six parts Oil Red O stock solution (0.5% w/v in isopropyl alcohol, Sigma-Aldrich, O-0625): four parts water] for 1 h at RT. Excess stain was removed by washing with water.

Assessment of triglyceride content. Cellular triglyceride (TG) content was evaluated after Oil Red O staining by spectrophotometric quantification, dissolving the stained lipid droplets in 100% 2-propanol for 10 min. Optical density of the extracts was then measured with a spectrophotometer Bio-Rad (iMark, Microplate Absorbance Reader) at 500 nm.

Isolation of total RNA and Real-Time PCR. Total RNA from tissues was extracted with Isol-RNA Lysis Reagent (5 PRIME, 2302700) according to manufacturer's instructions and retro-transcribed as previously described.[29]

Taq-Man quantitative PCR was performed on an ABI Prism 7700 Sequence Detection System (Applied Biosystems) using TATA-binding protein as control for equal loading. Predesigned mouse primers and probes were obtained from Applied Biosystems. Data were analyzed using the ΔΔ-ct method.

Isolation of gDNA. Fifty milligrams of frozen tissues (EPI and SC from CFD and HFD mice) were lysed using 200 μl of lysis buffer (10 mM TRIS HCl pH 8.8, 60 mM NaCl, 10 mM EDTA, 0.5% Triton X-100, Proteinase K 1 mg/ml). After incubation at 50°C for 4 h, samples were spun at 14,000 for 10', supernatants collected, phenol-chloroform-isoamyl alcohol extracted. gDNA was finally precipitated with 3 M sodium acetate and 2.5 volumes of ethanol. Quantification was performed using a BioRad spectrophotometer at 260 nm.

Statistical analysis. The number of mice in each experimental group is indicated in the figure legends. The two-tailed Student's t-test was used for paired comparisons. The chi-square test was employed to evaluate differences and calculate p values for cell size distributions; standardized residuals for each cell were calculated in order to determine the major contributors of global significance. The area values have been logarithmic transformed so as to correct the skewness of the distribution. Preliminary tests were also conducted to check for data normality and homogeneity of variances using the Kolmogorov-Smirnov and the Levene's tests, respectively. A significance limit of $p < 0.05$ was set. When specified, 2-way ANOVA followed by Bonferroni post-hoc tests for selected comparisons was used. All values are expressed as means ± SEM.

Disclosure of Potential Conflicts of Interest

No potential conflicts of interest were disclosed.

Acknowledgments

The authors want to thank Dr Franklin G. Berger for providing founders of the $Hp^{-/-}$ mouse colony. M. Maffei is an Associate Telethon Scientist. S.L. and M. Marchi are supported by a Telethon fellowship. This work was supported by the Telethon Foundation (TCP99016 to M. Maffei) and Italian ministry of education (20083ZAXYC_004 to F.S.).

References

1. Wang Y, Kinzie E, Berger FG, Lim SK, Baumann H. Haptoglobin, an inflammation-inducible plasma protein. Redox Rep 2001; 6:379-85; PMID:11865981; http://dx.doi.org/10.1179/135100001101536580
2. Friedrichs WE, Navarijo-Ashbaugh AL, Bowman BH, Yang F. Expression and inflammatory regulation of haptoglobin gene in adipocytes. Biochem Biophys Res Commun 1995; 209:250-6; PMID:7726843; http://dx.doi.org/10.1006/bbrc.1995.1496
3. Chiellini C, Bertacca A, Novelli SE, Görgün CZ, Ciccarone A, Giordano A, et al. Obesity modulates the expression of haptoglobin in the white adipose tissue via TNFalpha. J Cell Physiol 2002; 190:251-8; PMID:11807829; http://dx.doi.org/10.1002/jcp.10061
4. Chiellini C, Santini F, Marsili A, Berti P, Bertacca A, Pelosini C, et al. Serum haptoglobin: a novel marker of adiposity in humans. J Clin Endocrinol Metab 2004; 89:2678-83; PMID:15181041; http://dx.doi.org/10.1210/jc.2003-031965
5. Nielsen MJ, Moestrup SK. Receptor targeting of hemoglobin mediated by the haptoglobins: roles beyond heme scavenging. Blood 2009; 114:764-71; PMID:19380867; http://dx.doi.org/10.1182/blood-2009-01-198309
6. Maffei M, Funicello M, Vottari T, Gamucci O, Costa M, Lisi S, et al. The obesity and inflammatory marker haptoglobin attracts monocytes via interaction with chemokine (C-C motif) receptor 2 (CCR2). BMC Biol 2009; 7:87; PMID:20017911; http://dx.doi.org/10.1186/1741-7007-7-87
7. Lisi S, Gamucci O, Vottari T, Scabia G, Funicello M, Marchi M, et al. Obesity-associated hepatosteatosis and impairment of glucose homeostasis are attenuated by haptoglobin deficiency. Diabetes 2011; 60:2496-505; PMID:21873550; http://dx.doi.org/10.2337/db10-1536
8. Gustafson B. Adipose tissue, inflammation and atherosclerosis. J Atheroscler Thromb 2010; 17:332-41; PMID:20124732; http://dx.doi.org/10.5551/jat.3939
9. Maffeis C, Silvagni D, Bonadonna R, Grezzani A, Banzato C, Tatò L. Fat cell size, insulin sensitivity, and inflammation in obese children. J Pediatr 2007; 151:647-52; PMID:18035146; http://dx.doi.org/10.1016/j.jpeds.2007.04.053
10. Romanatto T, Roman EA, Arruda AP, Denis RG, Solon C, Milanski M, et al. Deletion of tumor necrosis factor-alpha receptor 1 (TNFR1) protects against diet-induced obesity by means of increased thermogenesis. J Biol Chem 2009; 284:36213-22; PMID:19858212; http://dx.doi.org/10.1074/jbc.M109.030874
11. Matthews VB, Allen TL, Risis S, Chan MH, Henstridge DC, Watson N, et al. Interleukin-6-deficient mice develop hepatic inflammation and systemic insulin resistance. Diabetologia 2010; 53:2431-41; PMID:20697689; http://dx.doi.org/10.1007/s00125-010-1865-y
12. Cawthorn WP, Heyd F, Hegyi K, Sethi JK. Tumour necrosis factor-alpha inhibits adipogenesis via a beta-catenin/TCF4(TCF7L2)-dependent pathway. Cell Death Differ 2007; 14:1361-73; PMID:17464333; http://dx.doi.org/10.1038/sj.cdd.4402127
13. Younce CW, Azfer A, Kolattukudy PE. MCP-1 (monocyte chemotactic protein-1)-induced protein, a recently identified zinc finger protein, induces adipogenesis in 3T3-L1 pre-adipocytes without peroxisome proliferator-activated receptor gamma. J Biol Chem 2009; 284:27620-8; PMID:19666473; http://dx.doi.org/10.1074/jbc.M109.025320
14. Fain JN, Madan AK, Hiler ML, Cheema P, Bahouth SW. Comparison of the release of adipokines by adipose tissue, adipose tissue matrix, and adipocytes from visceral and subcutaneous abdominal adipose tissues of obese humans. Endocrinology 2004; 145:2273-82; PMID:14726444; http://dx.doi.org/10.1210/en.2003-1336
15. do Nascimento CO, Hunter L, Trayhurn P. Regulation of haptoglobin gene expression in 3T3-L1 adipocytes by cytokines, catecholamines, and PPARgamma. Biochem Biophys Res Commun 2004; 313:702-8; PMID:14697247; http://dx.doi.org/10.1016/j.bbrc.2003.12.008
16. Herrera E, Amusquivar E. Lipid metabolism in the fetus and the newborn. Diabetes Metab Res Rev 2000; 16:202-10; PMID:10867720; http://dx.doi.org/10.1002/1520-7560(200005/06)16:3<202::AID-DMRR116>3.0.CO;2-#
17. Arner P. Human fat cell lipolysis: biochemistry, regulation and clinical role. Best Pract Res Clin Endocrinol Metab 2005; 19:471-82; PMID:16311212; http://dx.doi.org/10.1016/j.beem.2005.07.004
18. Mottagui-Tabar S, Rydén M, Löfgren P, Faulds G, Hoffstedt J, Brookes AJ, et al. Evidence for an important role of perilipin in the regulation of human adipocyte lipolysis. Diabetologia 2003; 46:789-97; PMID:12802495; http://dx.doi.org/10.1007/s00125-003-1112-x
19. Ray H, Pinteur C, Frering V, Beylot M, Large V. Depot-specific differences in perilipin and hormone-sensitive lipase expression in lean and obese. Lipids Health Dis 2009; 8:58; PMID:20017959; http://dx.doi.org/10.1186/1476-511X-8-58
20. Cid MC, Grant DS, Hoffman GS, Auerbach R, Fauci AS, Kleinman HK. Identification of haptoglobin as an angiogenic factor in sera from patients with systemic vasculitis. J Clin Invest 1993; 91:977-85; PMID:7680672; http://dx.doi.org/10.1172/JCI116319
21. Kratchmarova I, Kalume DE, Blagoev B, Scherer PE, Podtelejnikov AV, Molina H, et al. A proteomic approach for identification of secreted proteins during the differentiation of 3T3-L1 preadipocytes to adipocytes. Mol Cell Proteomics 2002; 1:213-22; PMID:12096121; http://dx.doi.org/10.1074/mcp.M200006-MCP200
22. van Tienen FH, van der Kallen CJ, Lindsey PJ, Wanders RJ, van Greevenbroek MM, Smeets HJ. Preadipocytes of type 2 diabetes subjects display an intrinsic gene expression profile of decreased differentiation capacity. Int J Obes (Lond) 2011; 35:1154-64; PMID:21326205; http://dx.doi.org/10.1038/ijo.2010.275
23. Roberts R, Hodson L, Dennis AL, Neville MJ, Humphreys SM, Harnden KE, et al. Markers of de novo lipogenesis in adipose tissue: associations with small adipocytes and insulin sensitivity in humans. Diabetologia 2009; 52:882-90; PMID:19252892; http://dx.doi.org/10.1007/s00125-009-1300-4
24. Jo J, Gavrilova O, Pack S, Jou W, Mullen S, Sumner AE, et al. Hypertrophy and/or Hyperplasia: Dynamics of Adipose Tissue Growth. PLoS Comput Biol 2009; 5:e1000324; PMID:19325873; http://dx.doi.org/10.1371/journal.pcbi.1000324
25. Miyoshi H, Perfield JW, 2nd, Obin MS, Greenberg AS. Adipose triglyceride lipase regulates basal lipolysis and lipid droplet size in adipocytes. J Cell Biochem 2008; 105:1430-6; PMID:18980248; http://dx.doi.org/10.1002/jcb.21964
26. Nishimura S, Manabe I, Nagasaki M, Hosoya Y, Yamashita H, Fujita H, et al. Adipogenesis in obesity requires close interplay between differentiating adipocytes, stromal cells, and blood vessels. Diabetes 2007; 56:1517-26; PMID:17389330; http://dx.doi.org/10.2337/db06-1749
27. Pasarica M, Sereda OR, Redman LM, Albarado DC, Hymel DT, Roan LE, et al. Reduced adipose tissue oxygenation in human obesity: evidence for rarefaction, macrophage chemotaxis, and inflammation without an angiogenic response. Diabetes 2009; 58:718-25; PMID:19074987; http://dx.doi.org/10.2337/db08-1098
28. Michailidou Z, Turban S, Miller E, Zou X, Schrader J, Ratcliffe PJ, et al. Increased angiogenesis protects against adipose hypoxia and fibrosis in metabolic disease-resistant 11β-hydroxysteroid dehydrogenase type 1 (HSD1)-deficient mice. J Biol Chem 2012; 287:4188-97; PMID:22158867; http://dx.doi.org/10.1074/jbc.M111.259325
29. Funicello M, Novelli M, Ragni M, Vottari T, Cocuzza C, Soriano-Lopez J, et al. Cathepsin K null mice show reduced adiposity during the rapid accumulation of fat stores. PLoS One 2007; 2:e683; PMID:17668061; http://dx.doi.org/10.1371/journal.pone.0000683
30. Müller G. Let's shift lipid burden–from large to small adipocytes. Eur J Pharmacol 2011; 656:1-4; PMID:21295025; http://dx.doi.org/10.1016/j.ejphar.2011.01.035
31. Villanueva CJ, Waki H, Godio C, Nielsen R, Chou WL, Vargas L, et al. TLE3 is a dual-function transcriptional coregulator of adipogenesis. Cell Metab 2011; 13:413-27; PMID:21459326; http://dx.doi.org/10.1016/j.cmet.2011.02.014
32. Hirata M, Suzuki M, Ishii R, Satow R, Uchida T, Kitazumi T, et al. Genetic defect in phospholipase Cδ1 protects mice from obesity by regulating thermogenesis and adipogenesis. Diabetes 2011; 60:1926-37; PMID:21617180; http://dx.doi.org/10.2337/db10-1500
33. Cinti S, Mitchell G, Barbatelli G, Murano I, Ceresi E, Faloia E, et al. Adipocyte death defines macrophage localization and function in adipose tissue of obese mice and humans. J Lipid Res 2005; 46:2347-55; PMID:16150820; http://dx.doi.org/10.1194/jlr.M500294-JLR200
34. Jo J, Guo J, Liu T, Mullen S, Hall KD, Cushman SW, et al. Hypertrophy-driven adipocyte death overwhelms recruitment under prolonged weight gain. Biophys J 2010; 99:3535-44; PMID:21112277; http://dx.doi.org/10.1016/j.bpj.2010.10.009
35. DeFuria J, Bennett G, Strissel KJ, Perfield JW, 2nd, Milbury PE, Greenberg AS, et al. Dietary blueberry attenuates whole-body insulin resistance in high fat-fed mice by reducing adipocyte death and its inflammatory sequelae. J Nutr 2009; 139:1510-6; PMID:19515743; http://dx.doi.org/10.3945/jn.109.105155
36. Lim SK, Kim H, Lim SK, bin Ali A, Lim YK, Wang Y, et al. Increased susceptibility in Hp knockout mice during acute hemolysis. Blood 1998; 92:1870-7; PMID:9731043